Cancer Research

Heme Oxygenase-1 Controls an HDAC4-miR-206 Pathway of Oxidative Stress in Rhabdomyosarcoma

Maciej Ciesla[1], Paulina Marona[1], Magdalena Kozakowska[1], Mateusz Jez[1], Marta Seczynska[1], Agnieszka Loboda[1], Karolina Bukowska-Strakova[1], Agata Szade[1], Magdalena Walawender[1], Magdalena Kusior[1], Jacek Stepniewski[1], Krzysztof Szade[1], Bart Krist[1], Oleksandr Yagensky[1], Aleksandra Urbanik[2], Bernarda Kazanowska[2], Jozef Dulak[1,3], and Alicja Jozkowicz[1]

Abstract

Rhabdomyosarcoma (RMS) is an aggressive soft tissue cancer characterized by disturbed myogenic differentiation. Here we report a role for the oxidative stress response factor HO-1 in progression of RMS. We found that HO-1 was elevated and its effector target miR-206 decreased in RMS cell lines and clinical primary tumors of the more aggressive alveolar phenotype (aRMS). In embryonal RMS (eRMS), HO-1 expression was induced by Pax3/7-FoxO1, an aRMS hallmark oncogene, followed by a drop in miR-206 levels. Inhibition of HO-1 by tin protoporphyrin (SnPP) or siRNA downregulated Pax3/7-FoxO1 target genes and induced a myogenic program in RMS. These effects were not mediated by altered myoD expression; instead, cells with elevated HO-1 produced less reactive oxygen species, resulting in nuclear localization of HDAC4 and miR-206 repression. HO-1 inhibition by SnPP reduced growth and vascularization of RMS tumors *in vivo* accompanied by induction of miR-206. Effects of SnPP on miR-206 expression and RMS tumor growth were mimicked by pharmacologic inhibition of HDAC. Thus, HO-1 inhibition activates an miR-206–dependent myogenic program in RMS, offering a novel therapeutic strategy for treatment of this malignancy. *Cancer Res; 76(19); 5707–18. ©2016 AACR.*

Introduction

Rhabdomyosarcoma is the most common soft tissue sarcoma in children and adolescents (1). Two main rhabdomyosarcoma subtypes are distinguished: embryonal (eRMS), with heterogeneous molecular fingerprint (2, 3), and alveolar (aRMS) characterized by the translocations t(2;13) or t(1;13) resulting in formation of fusion protein Pax3/7-FoxO1. This oncoprotein targets muscle markers like MyoD, apoptosis related kinases or epigenetic landscape sculpting proteins (4, 5). Pax3/7-FoxO1 plays a pivotal role in aRMS progression, increasing the expression of stromal cell–derived factor-1 (SDF1) and its receptor CXCR4 or hepatocyte growth factor (HGF) and its receptor cMET (6). Accordingly, the translocation-positive aRMS have poor prognosis, with early onset metastases (7).

Despite expression of promyogenic molecules, RMS does not fulfill myogenic program and remains highly proliferative (8). The central role in myogenesis plays myoD transcription factor (9), muscle-specific miRNAs (myomirs: miR-1, miR-133a, miR-133b, and miR-206), and ubiquitously expressed miRNAs from miR-29 family (10, 11).

We have shown that heme oxygenase-1 (HO-1, encoded by *HMOX1* gene), a cytoprotective, antioxidative, and proangiogenic heme-degrading enzyme promotes proliferation and impairs differentiation of myoblasts (12). HO-1 degrades heme to produce biliverdin, ferrous ion and carbon monoxide (CO) or can act trough protein–protein interaction with Nrf2 transcription factor (13, 14). The mechanism underlying the antimyogenic effect of HO-1 in myoblasts is CO-dependent inhibition of C/EBPδ binding to the myoD promoter that decreases myoD expression. In addition, HO-1 diminishes production of myomirs (12).

Expression of HO-1 is induced by oxidative stress, the effect mediated mainly by Nrf2. It can be upregulated by oncogenes, including cMET, thus its expression is often elevated in cancer (14, 15). Usually, activation of HO-1 in tumors increases resistance to oxidative stress, reduces apoptosis, and enhances angiogenesis (15). HO-1 is known to affect expression or activity of VEGF, HGF, or SDF1, and modulate activity of p38 kinases (15, 16).

HO-1 has been proposed as an aim in anticancer therapies (17). Here, we hypothesized that targeting HO-1 could inhibit

[1]Department of Medical Biotechnology, Faculty of Biochemistry, Biophysics and Biotechnology, Jagiellonian University, Krakow, Poland. [2]Department of Oncology, Hematology and Bone Marrow Transplantation, Wroclaw Medical University, Wroclaw, Poland. [3]International Associated Laboratory, Malopolska Centre of Biotechnology, Jagiellonian University, Krakow, Poland.

Note: Supplementary data for this article are available at Cancer Research Online (http://cancerres.aacrjournals.org/).

J. Dulak and A. Jozkowicz contributed equally to this article.

Corresponding Author: Alicja Jozkowicz, Faculty of Biochemistry, Biophysics and Biotechnology, Department of Medical Biotechnology, Jagiellonian University, Gronostajowa 7, Krakow 30-387, Poland. Phone: 481-2664-6411; Fax: 481-2664-6918; E-mail: alicja.jozkowicz@uj.edu.pl

doi: 10.1158/0008-5472.CAN-15-1883

progression of RMS through facilitating the myogenic differentiation and reducing angiogenesis and tumor growth.

We show that expression of HO-1 is induced by Pax3-FoxO1 and is elevated in aRMS cell lines and clinical tumors. Inhibition of HO-1 activity attenuates Pax3-FoxO1–dependent activation of SDF1 and HGF pathways, improves induction of differentiation of RMS cells through upregulation of miR-206 expression, reduces tumor growth, and decreases tumor vascularization.

Materials and Methods

Cell cultures

Rhabdomyosarcoma cell lines of embryonal (RD and SMS-CTR) and alveolar (CW9019, RH5, RH18, and RH28) origin were kindly provided by Dr. Peter Houghton (Nationwide Children's Hospital, Columbus, OH) in June 2009. To confirm cell line identities, known short tandem repeats were analyzed (Genmed, June 2015).

Cells were cultured in DMEM containing 25 mmol/L glucose (Lonza), with 10% FBS, penicillin (100 U/mL), and streptomycin (100 μg/mL; Gibco). For induction of differentiation, 5 days of culture in DMEM with 2% horse serum was used. Inhibition of HO-1 expression or activity was performed by siRNA (Ambion) or tin protoporphyrin (SnPP, 10 μmol/L). HDAC4 was inhibited by valproic acid (VA, 2 mmol/L), trichostatin A (20 nmol/L), or shRNA (Ambion). For reactive oxygen species (ROS) scavenging, N-acetyl cysteine (2 mmol/L) was used.

To silence or overexpress miR-206 commercially available sequences were chosen (Ambion). Pax3-FoxO1 construct was kind gift of Dr. Frederick Barr (National Cancer Institute, Bethesda, MD; ref. 18). Enzymatically active and mutated HO-1 constructs were courtesy of Dr. Makoto Suematsu (Keio University, Tokyo, Japan).

Functional assays

For quantification of oxidative stress, OxiSelect Total Antioxidant Capacity kit (Cell Biolabs) and 2′7′-dichlorofluorescein diacetate assay were used. For assessment of cell viability and proliferation, MTT reduction (Sigma) and modified fibrin bead assays were implied.

Animal models of tumor growth

FoxP3$^{Nu/Nu}$ mice (Harlan) were kept under SPF conditions, with water and food *ad libitum*.

Luciferase expressing genetically engineered SMS-CTR and CW9019 cells (12) were injected as a spheroid (SMS-CTR-Luc, 1000 cells in Matrigel) or cell suspension (CW9019-Luc, 1.5×10^6 cells in Matrigel) into the flank of mice. For SMS-CTR-Luc injection, animals were randomly divided into vehicle and SnPP groups at day 7 after transplantation. Intraperitoneal injections of SnPP (10 mg/kg) or vehicle were performed for two weeks every second day and tumor growth was followed for next week. For CW9019-Luc, intraperitoneal injections of SnPP, intratumoral injections of VA (100 mg/kg), or treatment with vehicles were performed every second day for three weeks, starting from day 14 after transplant. For shRNA experiments, SMS-CTR and CW9019 cells engineered with scrambled or HO-1 shRNA were injected into the flank of mouse (1.5×10^6 cells in Matrigel). Tumor growth was monitored for 12 (SMS-CTR) or 28 (CW9019) days.

Tumor growth was monitored using caliper measurements and luminescence imaging (IVIS Ilumina). Vascularization was examined by ultrasonography (VEVO2100). After tumor excision, RNA isolation or histologic analysis were performed.

Clinical samples

Primary, paraffin embedded specimens from collection of human rhabdomyosarcoma patients diagnosed with embryonal ($N = 15$) and alveolar ($N = 16$) RMS were sectioned and used for RNA isolation (Qiagen) or immunohistochemical staining.

Gene expression analysis

For gene expression analysis, qRT-PCR was used as described elsewhere (12). Western blotting was used for protein detection and immunohistochemical and ImageStream analysis implied for assessment of protein localization. Detailed procedures and lists of primers and antibodies are listed in Supplementary Material.

ImageStream analysis of protein localization

For analysis of HO-1 protein intracellular localization, the cells were harvested, fixed in 2% paraformaldehyde, and permeabilized in 0.2% Triton-X100. Staining was performed with antibody recognizing N-terminus of HO-1 (SPA-896, Enzo) and appropriate secondary antibody conjugated with Alexa-Fluor488 was used. Nuclei were counterstained with 7-AAD. Cell collection and analysis was performed using ImageStream image cytometer (Amnis).

Study approval

Mice were handled accordingly to regulations of national and local animal welfare bodies. All experiments were approved by the Local Ethics Committee (approval 39/2013 and 65/2013).

Statistical analysis

Results are shown as mean ± SEM. Number of experiments or number of animals are indicated in the figure legends. Two-tailed paired or unpaired Student *t* test or Mann–Whitney test were used for comparison of two groups. One-way ANOVA coupled with Tukey *post hoc* test was applied for multiple groups.

More detailed description of methods is provided as Supplementary Material.

Results

Gene expression signatures in embryonal and alveolar RMS

First set of experiments was performed in two human rhabdomyosarcoma cell lines: SMS-CTR (eRMS) and CW9019 (aRMS, carrying Pax7-FoxO1 mutation). Expressions of genes implicated in tumor progression, including cMET and its ligand HGF or CXCR4 and its ligand SDF1 were higher in aRMS than in eRMS (Fig. 1A and Supplementary Fig. S1). CW9019 and SMS-CTR showed also a slightly distinct sensitivity to cytostatics. Viability of eRMS but not aRMS cells was decreased after incubation with doxorubicin or cisplatin (Fig. 1B).

Expression of HO-1 in embryonal and alveolar RMS

Expression of SDF1 in myoblasts can be upregulated by HO-1 (12). HO-1 can also be a mediator of HGF/cMET pathway (19). Comparison of RMS cell lines showed decreased levels of miRNAs (miR-328, miR-338-3p, and miR-485-5p) targeting HO-1 (TargetScan base) in aRMS (Supplementary Fig. S2). Thus, we checked

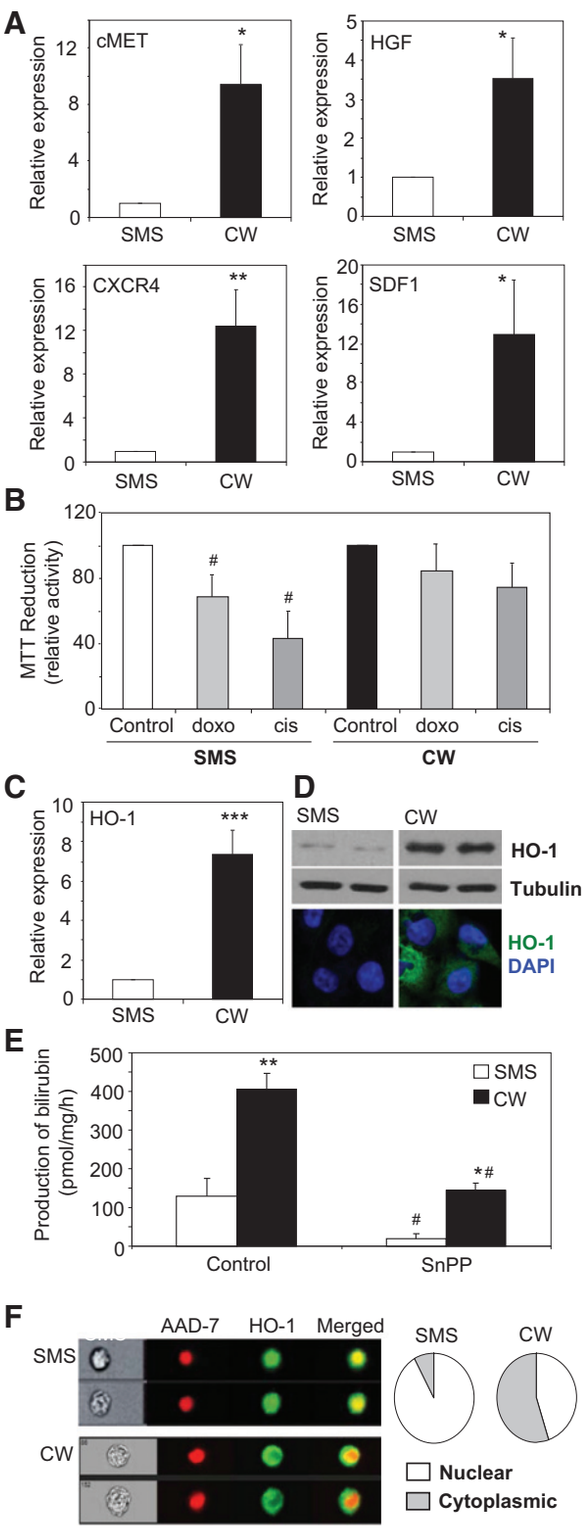

Figure 1.

Comparison of SMS-CTR (eRMS) and CW9019 (aRMS) cells. **A,** expression of cMET, *HGF*, *CXCR4*, and *SDF1* genes. Quantitative RT-PCR. $N = 9$–15. **B,** effect of doxorubicin (doxo) and cisplatin (cis) on cell viability after 48-hour culture. MTT reduction assay. $N = 3$. **C,** expression of HO-1 mRNA. Quantitative RT-PCR. EF2 served as internal control. $N = 26$. **D,** expression of HO-1 protein. Western blot analysis and immunofluorescent staining. Tubulin served as loading control. **E,** enzymatic activity of HO-1 in control and SnPP-treated cells. Colorimetric measurement of bilirubin. $N = 3$. **F,** intracellular localization of HO-1 protein. ImageStream analysis, representative pictures, and quantification. $N = 3$. AAD-7 was used to visualize nuclei. *, $P < 0.05$; **, $P < 0.01$; ***, $P < 0.001$ versus SMS-CTR; #, $P < 0.05$ versus control.

whether increased expression of CXCR4/SDF1 and cMET/HGF genes in aRMS is accompanied by upregulation of HO-1.

Indeed, expression of HO-1 was higher in CW9019 cell line at both transcript and protein level (Fig. 1C and D) followed by higher enzymatic activity (Fig. 1E). Noteworthy, HO-1 protein in RMS was present not only in cytoplasm but also in nucleus (Fig. 1F), where HO-1 is supposed to act independently of its enzymatic activity (20).

To verify whether HO-1 is merely coexpressed with CXCR/SDF1 and cMET/HGF or it can also influence their production, HO-1 was blocked by SnPP. Inhibition of HO-1 activity reduced expression of all four genes (Supplementary Fig. S3A), indicating that effects of HO-1 rely on its enzymatic function. HGF- and SDF1-dependent pathways are known to stimulate the proliferation of myoblasts while inhibiting their differentiation (21). Indeed, SnPP abolished the proliferation of both SMS-CTR and CW9019 cells (Supplementary Fig. S3B) and reduced the growth of both cell lines (Supplementary Fig. S3C).

Effect of Pax3-FoxO1 fusion protein on HO-1 expression

Characteristic features of aRMS are chromosomal translocations leading to the formation of Pax3/7-FoxO1 fusion genes. To check whether increased expression of HO-1 in aRMS may result from activity of these aberrant transcription factors, we transfected the SMS-CTR and CW9019 cell lines with Pax3-FoxO1 (Fig. 2A).

Introduction of fusion gene into eRMS cell line resulted in upregulation of HO-1 transcript (Fig. 2B) and protein (Fig. 2C). Interestingly, despite higher transfection efficacy (Fig. 2A), the same treatment did not modify the expression of HO-1 in CW9019 cells, which harbors the t(1;13) translocation and expresses Pax7-FoxO1 (Fig. 2B and C). Thus, we postulate the existence of a threshold level above which the pathway cannot be further influenced.

Upregulation of HO-1 is not observed until 48 hours after transfection of SMS-CTR with Pax3-FoxO1 (Supplementary Fig. S3D). This suggests an indirect influence on HO-1 expression, as Pax3-FoxO1 target genes were shown to respond rapidly (22). Accordingly, HO-1 promoter does not contain binding site for Pax3 (ENCODE data base) responsible for transcriptional activity of Pax3-FoxO1 (23).

Trying to determine the pathway underlying HO-1 upregulation, we focused on AP2 transcription factors. AP2β is a direct target of Pax3-Fox1 (24), while AP2δ directly regulates HO-1 expression (25). Therefore, we checked the effect of Pax3-FoxO1 on AP2δ. In both SMS-CTR and CW9019 cells, transfection with Pax3-FoxO1 led to increased expression of AP2δ (respectively 2.6 ± 0.51 and 3.6 ± 0.84 fold of induction in SMS-CTR and CW9019, $P = 0.048$ in both cell lines). However, knockdown of AP2δ in SMS-CTR did not influence

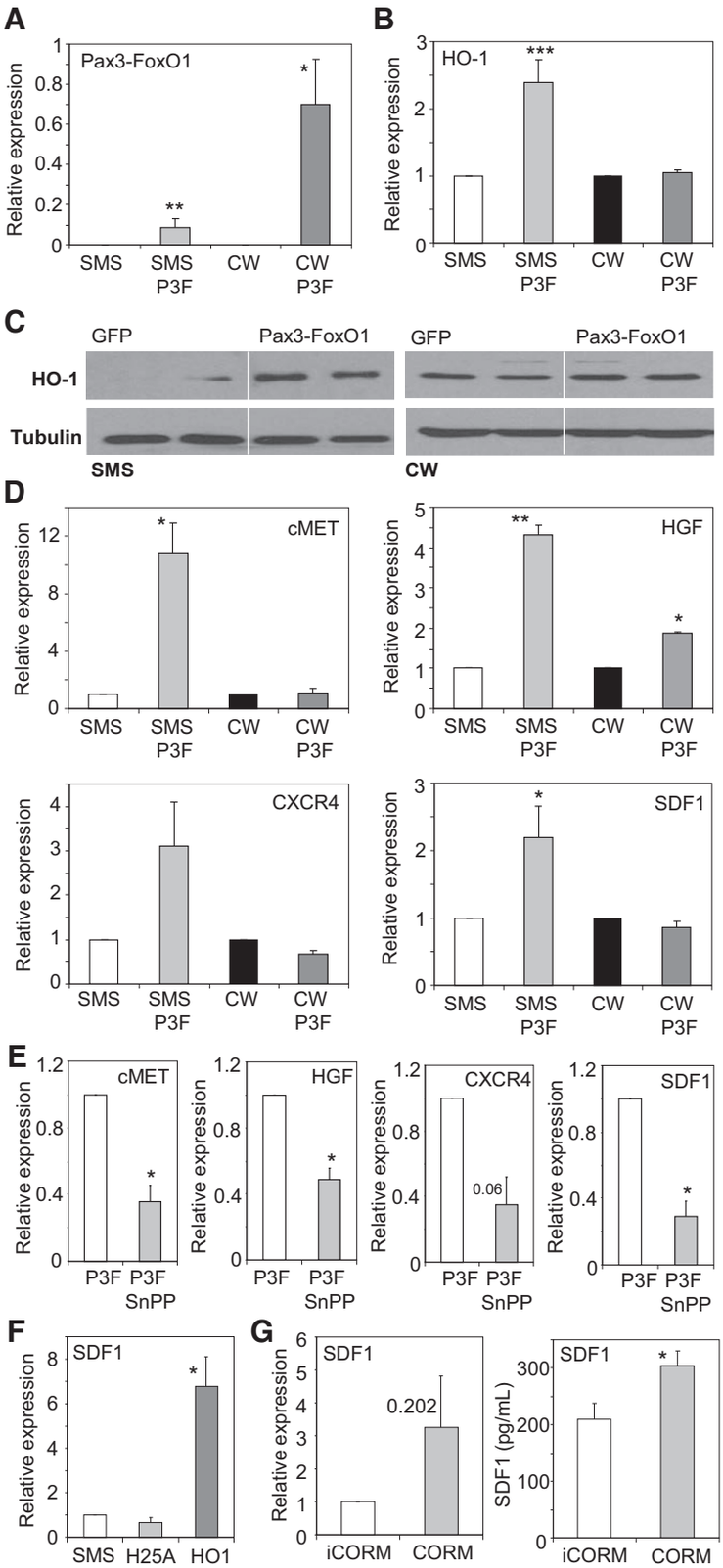

Figure 2.

Effects of transfection of SMS-CTR (eRMS) and CW9019 (aRMS) with Pax3-FoxO1 fusion gene (P3F). GFP served as control. **A,** expression of Pax3-FoxO1 mRNA. $N = 4$. **B,** expression of HO-1 mRNA. Quantitative RT-PCR. EF2 served as internal control. $N = 5$. **C,** expression of HO-1 protein. Western blot analysis. Tubulin served as loading control. **D,** expression of cMET, HGF, CXCR4, and SDF1 mRNAs in SMS-CTR and CW9019 cells. $N = 3$–8. **E,** effect of SnPP (24 hours) on the expression of cMET, HGF, CXCR4, and SDF1 mRNAs in SMS-CTR cells transfected with P3F. $N = 3$. **F,** effect of transfection of SMS-CTR cells with enzymatically active (HO1) or inactive HO-1 mutant (H25A) on expression of SDF1. $N = 3$. **G,** effect of carbon monoxide releasing molecule (CORM) on expression of SDF1 mRNA and secretion of SDF1 protein. Inactive CORM (iCORM) served as a control. Quantitative RT-PCR (EF2 served as internal control) and ELISA. $N = 3$. *, $P < 0.05$; **, $P < 0.01$; ***, $P < 0.001$ versus control.

induction of HO-1 by Pax3-FoxO1 (respectively 3.6 ± 1.83 and 3.5 ± 0.02 fold of induction in cells transfected with scrambled and AP2δ shRNA, $P = 0.482$).

Similar pattern of expression as for HO-1 was observed for cMET, CXCR4, and SDF1 upon Pax3-FoxO1 transfection (Fig. 2D). These genes were upregulated in response to oncoprotein in SMS-CTR but not CW9019, with only HGF increased in both cell lines, but to a lower extent in CW9019 (Fig. 2D). Higher expression of cMET, HGF, CXCR4, and SDF-1 in SMS-CTR cells transfected with Pax3-FoxO1 were reversed by HO-1 inhibition (Fig. 2E). Importance of HO-1 activity was confirmed by observation that only enzymatically proficient form and not its catalytically inactive mutant, upregulated SDF1 (Fig. 2F). We suppose that HO-1 may act through formation of carbon monoxide, as CO donor led to increased expression of SDF1 (Fig. 2G).

Expression of differentiation markers in embryonal and alveolar RMS cell lines

In standard culture conditions, CW9019 cells displayed lower expression of myomirs (miR-206, miR-133b), and miR-29b/c, in comparison with SMS-CTR cells (Fig. 3A). Accordingly, expression of differentiation markers, such as myogenin and myosin heavy chain (MyHC), was lower in CW9019 cells (Fig. 3B). Differentiation medium led to more myogenic phenotype of SMS-CTR, but not CW9019 cells, as illustrated by MyHC staining (Fig. 3C). HO-1 did not change significantly ($P > 0.120$ and $P > 0.095$ for SMS-CTR and CW9019, respectively) upon differentiation (Fig. 3D).

Earlier, we demonstrated that overexpression of HO-1 in myoblasts downregulates myoD (12). However, expression of myoD was comparable between SMS-CTR and CW9019 cells despite differences in HO-1 (Supplementary Fig. S4A). This may not reflect the activity of myoD, as in CW9019 cells, we found elevated level of myoR, a myoD repressor, accompanied by reduced expression of miR-378 that targets myoR (Supplementary Fig. S4B). Myogenic differentiation can also be modified by p38 kinases—while p38α seems indispensable for myogenesis, p38γ phosphorylates myoD and decreases its activity (26). In CW9019 cells, we detected less p38α and more p38γ isoform compared with SMS-CTR cells (Supplementary Fig. S4C). SnPP treatment did not affect either myoR and miR-378 expression or p38α protein level (Supplementary Fig. S4D and S4E). However, in aRMS, SnPP decreased the level of p38γ kinase, suggesting that HO-1 may influence p38γ-dependent circuitry (Supplementary Fig. S4E).

Effect of SnPP on expression of differentiation markers

CW9019 cells expressed lower levels of myogenic markers in both standard and differentiating conditions (Fig. 3). In particular, expression of miR-206 was increased in SMS-CTR but not in CW9019 cells upon differentiation (Fig. 4A). Inhibition of HO-1 further upregulated miR-206 in eRMS, and restored response to myogenic stimuli in aRMS cells (Fig. 4B). Similar pattern was observable for miR-133b, that is transcribed together with miR-206, whereas upregulation of miR-29c in SMS-CTR was not modified by SnPP (Fig. 4A and B). Concomitantly, expressions of myoD, myogenin, and MyHC tended to be increased in differentiated SMS-CTR (Fig. 4C), especially in presence of SnPP (Fig. 4D). Such a treatment was less effective in CW9019 cells.

Taken together, differentiation capabilities of CW9019 cells highly expressing HO-1 were impaired in comparison with SMS-CTR with lower level of HO-1. Inhibition of HO-1 in the RMS cells cultured in a myogenesis-promoting environment

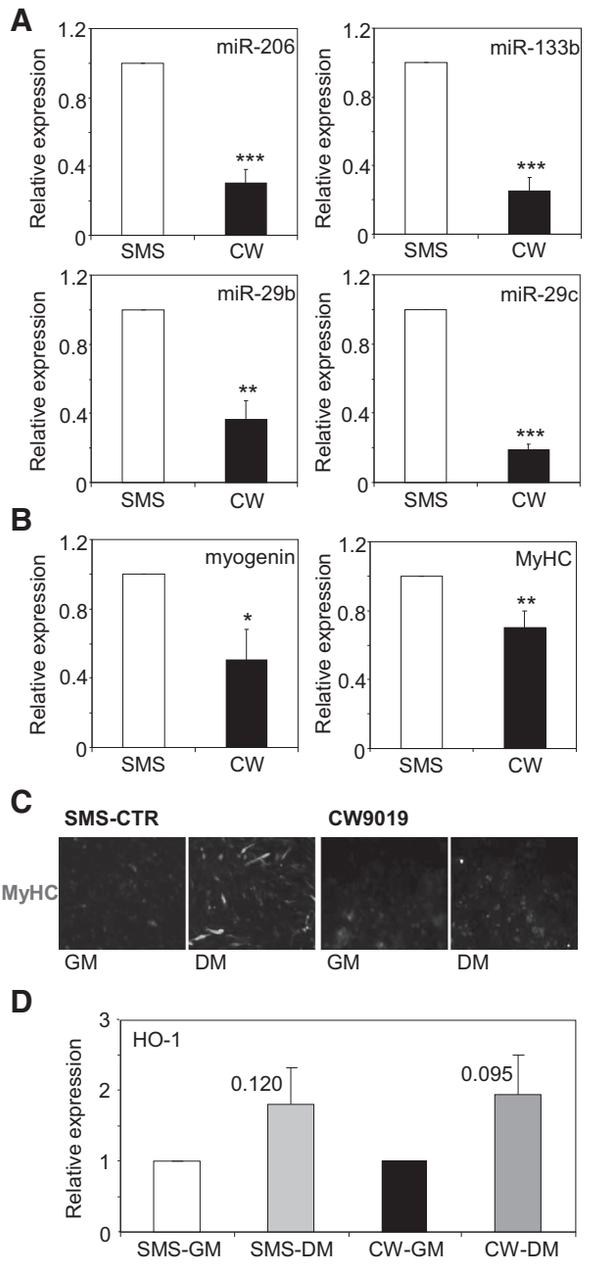

Figure 3.

Differentiation potential of SMS-CTR (eRMS) and CW9019 (aRMS) cell lines. **A,** expression of miR-206, miR-133b, miR-29b, and miR-29c in cells cultured in growth medium (GM). $N = 8–21$. **B,** expression of myogenin and MyHC in cells cultured in growth medium. Quantitative RT-PCR. U6 (**A**) and EF2 (**B**) served as internal control. $N = 16–20$. **C,** expression of MyHC protein in cells cultured in growth medium or in differentiation medium (DM). Immunofluorescent staining. **D,** effect of culture in differentiation medium on expression of HO-1. Quantitative RT-PCR. EF2 served as internal control. $N = 12–19$. *, $P < 0.05$; **, $P < 0.01$; ***, $P < 0.001$ versus SMS-CTR.

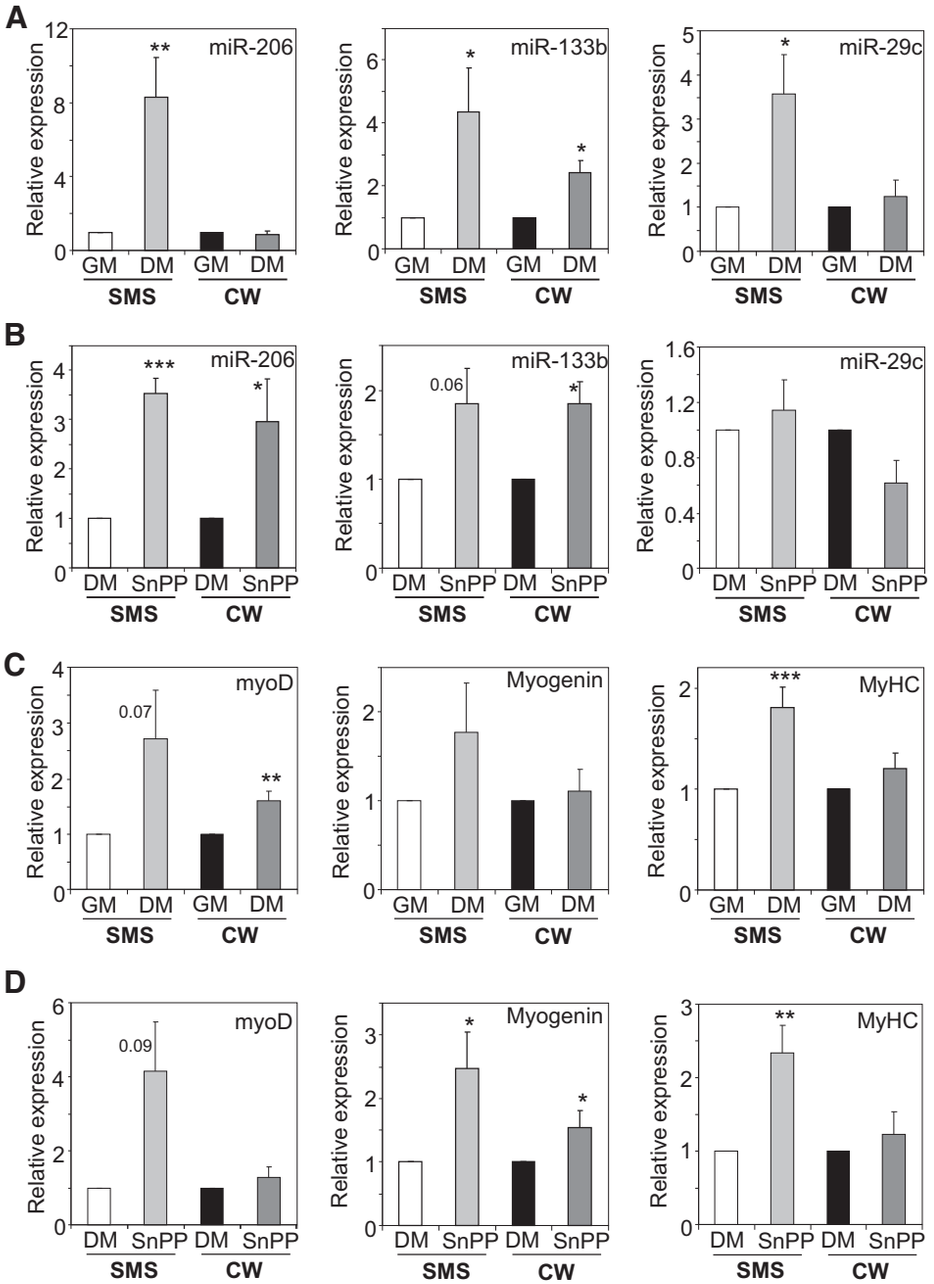

Figure 4.
Expression of differentiation markers in SMS-CTR (eRMS) and CW9019 (aRMS) cell lines cultured in differentiation medium (DM) with or without SnPP (10 μmol/L, 5 days). **A,** expression of miR-206, miR-133b, and miR-29c in cells cultured in differentiation medium. $N = 6$–26. **B,** effect of SnPP on expression of miR-206, miR-133b, and miR-29c in cells cultured in differentiation medium. $N = 2$–16. **C,** expression of myoD, myogenin, and MyHC in cells cultured in differentiation medium. $N = 10$–27. **D,** effect of SnPP on expression of myoD, myogenin, and MyHC in cells cultured in differentiation medium. $N = 3$–11. Quantitative RT-PCR. U6 (**A** and **B**) and EF2 (**C** and **D**) served as internal control. *, $P < 0.05$; **, $P < 0.01$; ***, $P < 0.001$ versus growth medium (GM; **A** and **C**) or control differentiation medium (**B** and **D**). Values of $P < 0.1$ are indicated.

facilitated the initiation of differentiation, particularly the upregulation of miR-206. We hypothesize that HO-1 activity may impede the myogenic differentiation of RMS due to inhibition of miR-206.

Role of miR-206 in RMS differentiation pathways

To check whether inhibition of miR-206 mediates the antimyogenic effect of HO-1 in Pax3/7-FoxO1–expressing cells, we introduced miR-206 into CW9019 cells. This resulted in upregulation of myogenin, without affecting MyHC expression (Supplementary Fig. S5A). Thus, miR-206 may initiate differentiation but is not sufficient to govern the later stages of myogenesis in aRMS. Accordingly, in SMS-CTR cells, where transfection with Pax3-FoxO1 downregulated miR-206, myogenin and MyHC (Supplementary Fig. S5B), myogenin but not MyHC expression was rescued by delivery of miR-206 (Supplementary Fig. S5B).

Because inhibition of HO-1 upregulated miR-206, myogenin, and MyHC in SMS-CTR cells (Fig. 4B and D), we analyzed the effect of miR-206 silencing. As shown in Supplementary Fig. S5C, antagomirs effectively silenced miR-206, what was accompanied by decreased expression of myogenin and MyHC both in control and SnPP-treated cells. Hence, miR-206 may be a nexus that regulates both differentiation and proliferation of RMS cells. Overexpression of miR-206 upregulated promyogenic pathways and downregulated SDF1 in

CW9019 cells (Supplementary Fig. S5D). Also cMET receptor was reduced in CW9019 at protein level upon miR-206 transfection (Supplementary Fig. S5D). That observation stays in accordance with previous reports (27) and with fact that 3′UTR of cMET contains miR-206–binding site (microrna.org database). Taken together, our results indicate that miR-206 initiates differentiation program while downregulating SDF1 and cMET in RMS. Thus, inhibition of miR-206 can mediate some effects of antimyogenic and proproliferative activity of HO-1.

Effect of oxidative stress on expression of miR-206

Expression of miR-206 can be downregulated by HDAC4 histone deacetylase. Under oxidative stress, HDAC4 is oxidized and exported to cytoplasm to derepress miR-206 (28). We hypothesized that such mechanism may be active in RMS. To verify this supposition, we compared oxidative status of SMS-CTR (with high expression of miR-206) and CW9019 cells (with low miR-206). The CW9019 displayed higher total antioxidative capacity and lower production of ROS than SMS-CTR (Fig. 5A and B). Reduction of oxidative stress in SMS-CTR cells led to downregulation of miR-206 (Fig. 5C). Accordingly, we observed increased HDAC4 immunostaining in aRMS in comparison to eRMS (Fig. 5D), and higher level of HDAC4 in SMS-CTR cells treated with ROS scavenger (Fig. 5E).

HO-1 is an antioxidative enzyme (14) but may also act independently of enzymatic activity, via interaction with several nuclear proteins (13). As HO-1 was present both in cytoplasm and nucleus of RMS cells (Fig. 1E), we examined whether HO-1 activity is necessary to inhibit miR-206. To this end, we transduced SMS-CTR cells with wild-type (active) or mutated (enzymatically inactive) form of *HMOX1*. Only introduction of wild-type *HMOX1* led to downregulation of miR-206 (Fig. 5F).

Our results indicate that activation of HO-1 reduces oxidative stress to maintain nuclear HDAC4 and thereby downregulates miR-206. Inhibition of HO-1 led to removal of HDAC4 from the nuclei of CW9019 cells (Fig. 5G and H) and to increased miR-206 expression (Fig. 5I). Similar increase was induced by VA, an HDACs inhibitor (Fig. 5I). Interestingly, the influence of trichostatin A, a pan-HDAC inhibitor, was weak (Fig. 5J), whereas specific genetic knockdown of HDAC4 led to upregulation of miR-206 expression (Fig. 5K), indicating that miR-206 is specifically regulated by HDAC4 in RMS.

Effect of HO-1 on the other RMS cell lines

As no universal conclusion can be driven solely from comparison of two cell lines, we repeated the most important analyzes in set of human RMS lines, namely RD (eRMS) and RH5, RH18 and RH28 (aRMS). In accordance with earlier observations (12), the expression of HO-1 mRNA was higher in RH5, RH18, and RH28 aRMS than in RD eRMS cells (Supplementary Fig. S6A). Similar difference was observable for cMET, significantly upregulated in aRMS lines (Supplementary Fig. S6B). Importantly, knockdown of HO-1 in RH18 cells reduced expression of cMET and increased expression of miR-206 (Supplementary Fig. S6C). Like in CW9019 and SMS-CTR cells, inhibition of HO-1 activity led to reduced proliferation of aRMS (Supplementary Fig. S6D) and increased maturation of eRMS (Supplementary Fig. S6E), as demonstrated for RH28 and RD cell lines, respectively. Culture of cells with SnPP upregulated the expression of myogenin (Supplementary Fig. S6F) and miR-206 (Supplementary Fig. S6G). Again, effect of SnPP on miR-206 in RD cells was comparable with that of VA (Supplementary Fig. S6G).

Effect of SnPP on growth of RMS tumors

To confirm the role of HO-1 in RMS development *in vivo*, we performed two experiments using cells engineered to express luciferase (SMS-CTR-Luc and CW9019-Luc). In the first, single spheroids of SMS-CTR-Luc cells were transplanted into athymic mice, subsequently treated with SnPP or vehicle. As shown in Fig. 6A, tumors from the SnPP-treated group were smaller not only during the administration but also after withdrawal of treatment. Measurements of tumor volume were confirmed by analysis of luciferase activity (Fig. 6A). In the second experiment, we transplanted subcutaneously the suspension of CW9019-Luc cells. Also, here inhibition of HO-1 resulted in decreased tumor growth (Fig. 6B), accompanied by higher expression of miR-206, miR-133b, and a tendency toward upregulation of MyHC (Fig. 6C).

Thus, systemic inhibition of HO-1 activity may reduce tumor growth and facilitate differentiation of RMS cells *in vivo*. That supposition was strengthened by observation that expressions of HO-1 and MyHC were mutually exclusive: cells positive for HO-1 were negative for MyHC and vice versa (Supplementary Fig. S7A). Tumors from SnPP-treated animals were also morphologically more heterogeneous and more fibrotic (Supplementary Fig. S7B). Moreover, comparison of the tumors with different growth kinetics within the control group (Supplementary Fig. S7C) revealed higher HO-1 and lower miR-206 expressions in fast-growing tumors (Supplementary Fig. S7D). Finally, inhibition of HO-1 decreased the tumor vascularization as shown by CD31 staining (Supplementary Fig. S7E) and ultrasonography (Supplementary Fig. S7F).

Apart from systemic inhibition of HO-1, we checked the effect of knockdown of HO-1 specifically in RMS cells. Genetic engineering of SMS-CTR and CW9019 cell lines with specific shRNA efficiently decreased the HO-1 expression (Fig. 6D and E) and led to the upregulation of miR-206 in tumors formed by both cell lines (Fig. 6F and G). Genetic inhibition of HO-1 and resulting upregulation of miR-206 was accompanied by reduced growth of eRMS (Fig. 6H), but not aRMS tumors (Fig. 6I). The difference between efficacy of systemic (by SnPP) and local (by shRNA) HO-1 inhibition may suggest off-target activity of SnPP, or indicate that not only HO-1 expressed by RMS cells, but also HO-1 from surrounding stromal cells may modulate the tumor growth (Supplementary Fig. S8).

In addition, we demonstrated that treatment of CW9019 tumors with VA evoked similar effects as administration of SnPP. Such tumors were smaller, displayed more heterogeneous morphology, and showed a tendency toward increased expression of miR-206, miR-133b, or MyHC (Supplementary Fig. S9A and S9B).

Expression of HO-1 and miR-206 in clinical RMS tumors

To check whether reported results have a relevance in clinical setting, we analyzed the expression of HO-1 in collection of primary RMS specimens. Quantitative RT-PCR showed increased HO-1 mRNA in aRMS when compared with eRMS tumors (Fig. 7A). This was supported by stronger immunohistochemical staining for HO-1 (Fig. 7A). In accordance to the *in vitro* and *in vivo* models, increased expression of HO-1 in aRMS

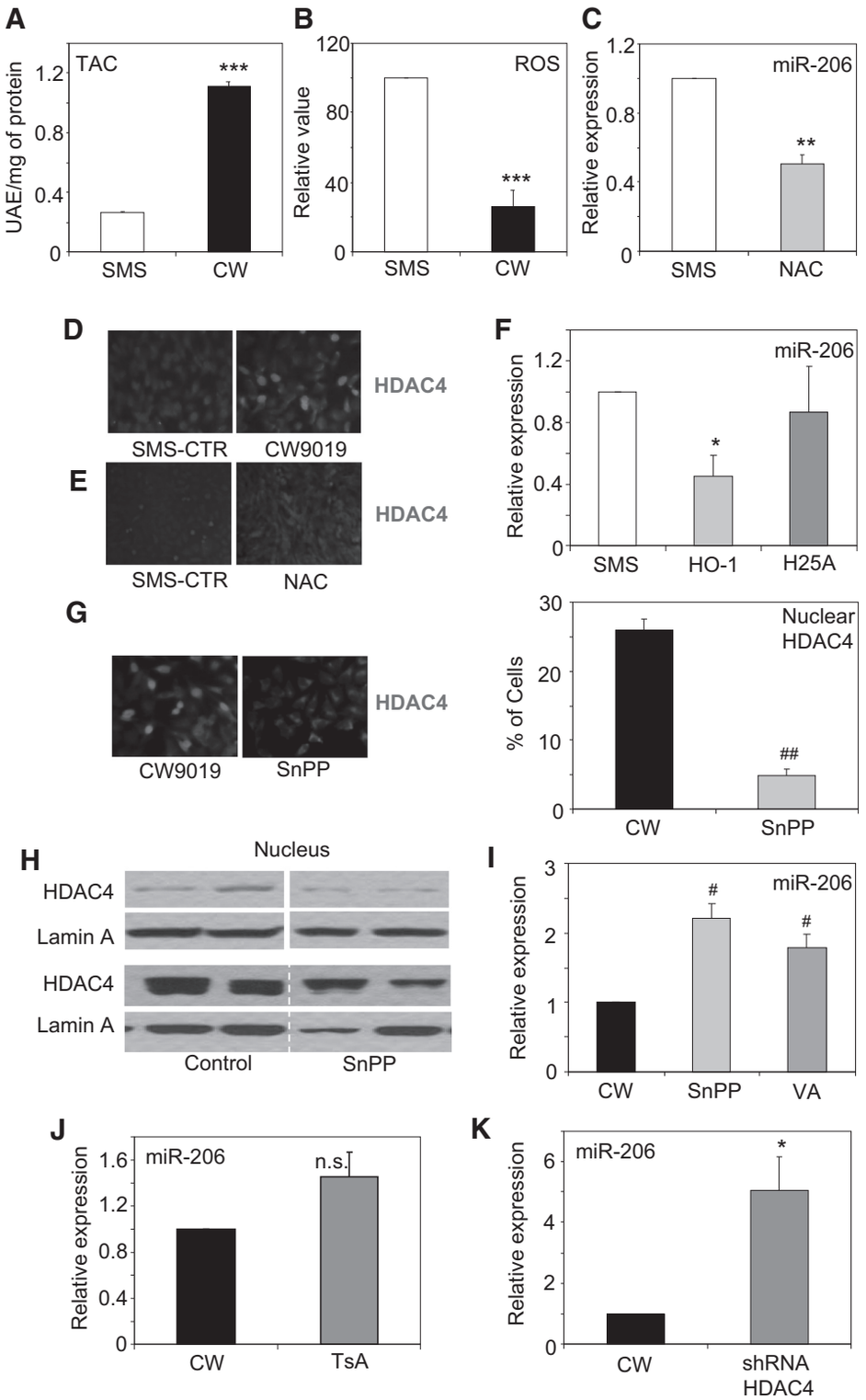

Figure 5.

Effect of oxidative stress in SMS-CTR (eRMS) and CW9019 (aRMS) cells cultured in standard conditions. **A,** total antioxidant capacity (TAC) in SMS-CTR and CW9019. Colorimetric assay. $N = 3$. **B,** ROS production in SMS-CTR and CW9019. Flow cytomeric analysis of DCF fluorescence. $N = 4$. **C,** effect of NAC (5 days) on expression of miR-206 in SMS-CTR cells cultured in differentiation conditions. Quantitative RT-PCR. $N = 4$. **D,** comparison of HDAC4 expression. **E,** effect of NAC (2 mmol/L, 24 hours) on expression of HDAC4 in SMS-CTR cells. Immunofluorescent staining. **F,** expression of miR-206 in SMS-CTR transfected with active (HO-1) and inactive (H25A) form of HO-1. Quantitative RT-PCR. $N = 4$. **G,** effect of SnPP (24 hours) on nuclear localization of HDAC4 in CW9019 cells. Immunofluorescent staining. **H,** effect of SnPP on nuclear localization of HDAC4 in CW9019 cells. Representative Western blots. Lamin A served as a loading control for nuclear fraction. **I,** effect of SnPP (5 days) and valproic acid (VA, 5 days) on the expression of miR-206. Quantitative RT-PCR. $N = 4$. **J,** effect of trichostatin A (TsA, HDAC inhibitor, 48 hours) on expression of miR-206 in CW9019 cells. $N = 3$. **K,** effect of HDAC4 shRNA knockdown on expression of miR-206 in CW9019 cells. Quantitative RT-PCR. U6 served as internal control. $N = 3$. *, $P < 0.05$; **, $P < 0.01$; ***, $P < 0.001$ versus SMS; #, $P < 0.05$; ##, $P < 0.01$ versus CW. n.s., nonsignificant.

was accompanied by higher vascularization (Fig. 7B), and lower expression of miR-206 (Fig. 7C). We also detected lower levels of miR-29a and miR-378 without significant decrease of miR-133b in aRMS (Fig. 7C). Taken together, analysis of clinical samples indicates association between higher expression of HO-1, decreased expression of miR-206, and elevated vascularization that may be clinically relevant in RMS progression.

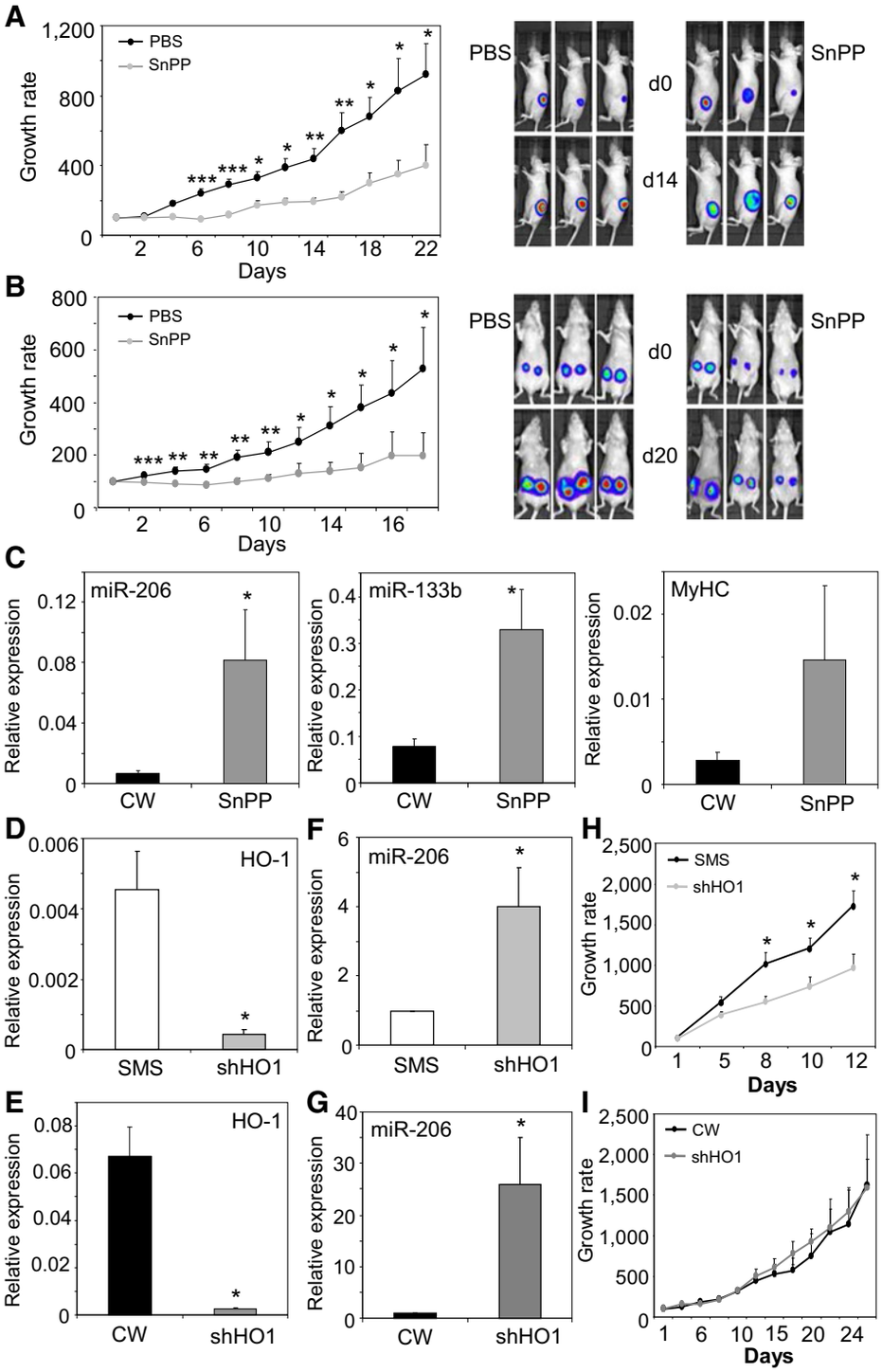

Figure 6.
Effect of SnPP on growth of tumors after subcutaneous transplantation of SMS-CTR-Luc eRMS or CW9019-Luc aRMS cells to immunodeficient mice. **A,** effect of SnPP on growth of tumors from SMS-CTR-Luc spheroids. $N = 6$–8. **B,** effect of SnPP on growth of tumors from CW9019-Luc cell suspensions. Caliper measurements of tumor volume and IVIS detection of luciferase activity. $N = 6$–8. **C,** expression of miR-206, miR-133b, and MyHC in tumors formed by CW9019-Luc cells. Quantitative RT-PCR. U6 (for miRNA) or EF2 (for MyHC) served as constitutive control. $N = 6$–8. **D** and **E,** knockdown of HO-1 after lentiviral delivery of shRNA to SMS-CTR (**D**) or CW9019 (**E**) cells used for *in vivo* experiment. $N = 3$. **F** and **G,** expression of miR-206 in rhabdomyosarcoma tumors formed by SMS-CTR (**F**) or CW9019 (**G**) cells after injection into immunodeficient mice. Tumors were collected 12 (SMS) or 28 (CW) days later. Quantitative RT-PCR. Actin (**D** and **E**) and U6 (**F** and **G**) served as constitutive control. $N = 6$–8. **H** and **I,** effect of HO-1 knockdown in SMS-CTR (**H**) or CW9019 (**I**) cells on growth of tumors after subcutaneous injection into immunodeficient mice. Caliper measurements. $N = 6$–8. *, $P < 0.05$; **, $P < 0.01$; ***, $P < 0.001$ versus control.

Discussion

In earlier study, we demonstrated that overexpression of HO-1 blocks myogenesis by inhibiting cEBPδ-dependent transcription of myoD and downregulating myomirs (12). Here we show that HO-1 also affects myogenic maturation of rhabdomyosarcoma. HO-1 is upregulated in the alveolar RMS and its elevated activity attenuates initiation of myogenic program in RMS, targeting miR-206 independently of myoD (Supplementary Fig. S10).

We report that in aRMS cell lines carrying Pax7-FoxO1 or Pax3-FoxO1, as well as in eRMS cells transfected with Pax3-FoxO1, the high level of HO-1 is accompanied by low expression of miR-206. Both pharmacologic inhibition and genetic silencing of HO-1 upregulate miR-206. Furthermore, only eRMS cells respond to promyogenic stimuli by induction of

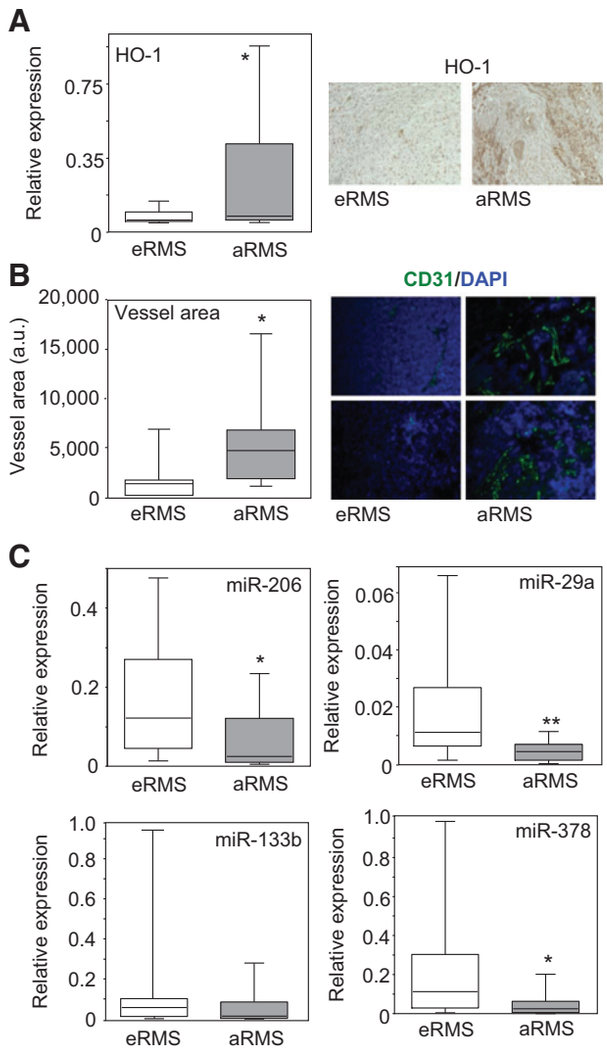

Figure 7.

Analysis of tumor tissue specimens from patients with eRMS ($N = 15$) and aRMS ($N = 16$). **A,** expression of HO-1 mRNA and protein. Quantitative RT-PCR (β-actin served as internal control) and immunohistochemical staining. **B,** vascularization of tumors. Quantitative analysis of $CD31^+$ area. Immunofluorescent staining. **C,** expression of miR-206, miR-133b, miR-29a, and miR-378. Quantitative RT-PCR. U6 served as internal control. *, $P < 0.05$; **, $P < 0.01$ versus eRMS.

differentiation and upregulation of miR-206 or myogenin. Inhibition of HO-1 restores this process, although only to some point, also in aRMS. In eRMS inhibition of HO-1, accompanied by further upregulation of miR-206, is even more effective and results in enhanced expression of late-differentiation markers, like MyHC.

Pax3/7-FoxO1 is an indicator of poor prognosis in aRMS (18). Both Pax3-FoxO1 and Pax7-FoxO1 are more active than Pax3 and Pax7 (8) and augment expression of CXCR4, SDF1, cMET, and HGF, proteins facilitating aRMS progression (6). HGF and cMET increase RMS proliferation and invasion while reduce apoptosis, correlating with increased aggressiveness of tumors (29). Transfection of eRMS with Pax3-FoxO1 increased growth and accelerated tumor formation in mice (8, 30). We showed that introduction of Pax3-FoxO1 into eRMS upregulated CXCR4/SDF1 and cMET/HGF genes, the effect attenuated by HO-1 inhibition.

HO-1 in myoblasts decreased expression of myoD, myogenin, and miR-206 (12). In accordance, high level of HO-1 in aRMS was accompanied by low levels of myogenin and miR-206, however, without affecting myoD expression. That may stem from distinct regulation of myoD in myoblasts and RMS. In myoblasts, the major factor governing the myoD transcription is cEBPδ (31). In translocation-positive RMS, myoD is directly regulated by Pax3/7-FoxO1 (5, 22, 32) and this interaction possibly outweighs inhibitory influence of HO-1. Importantly, Pax3/7-FoxO1 increases myoD expression, but impairs its function (33), and myoD expression in RMS does not correlate with clinical outcomes (8, 34).

In myoblasts, upmodulation of miR-378 facilitates myogenic differentiation by targeting myoD antagonist, myoR (35), with disturbances of this pathway observed in RMS (8, 36). Indeed, we found a decreased level of miR-378 and enhanced expression of myoR in aRMS in comparison with eRMS. These differences were, however, independent of HO-1 activity.

MyoD function is also regulated by p38 kinase isoforms. The p38α promotes myoD-E47 heterodimerization favoring differentiation (37, 38). In contrast, p38γ kinase reduces activity of myoD (26). We found increased expression of p38γ and lower of p38α in aRMS in comparison with eRMS, with inhibition of HO-1 affecting only p38γ, suggesting that HO-1 may in this way influence myoD activity.

In skeletal muscle, expression of miR-206/miR-133b is directly regulated by myoD and myoR (8). While miR-206 is expressed from its own promoter already in proliferating myoblasts, miR-133b is cotranscribed with linc-MD1 RNA upon differentiation (39). MyoD interacts genome-wide with histone acetyltransferases and deacetylases, but Pax3/7-FoxO1 can prevent chromatin remodeling at myoD target genes (8, 33). For example, at the myogenin locus, Pax3-FoxO1 diminishes the acetylation of histone H4 and the occupancy of RNA polymerase II (33). Promoters of miRNA genes are also epigenetically regulated by histone modifications (40) with promoter hypoacetylation playing a causal role in suppression of miR-206 in lung cancer (28).

In particular, HDAC4 can lead to gene repression through deacetylation of the lysine residues in histone H4 (41–43). HDAC4, belonging to class IIa HDACs, is enriched in heart and skeletal muscle where it inhibits myogenesis (43, 44). High levels of HDACs were reported in many cancers, although there is no data for RMS (44). Nevertheless, Oncomine database (Oncomine.org) analysis of Baird sarcoma data (45) indicates that HDAC4 is enriched in RMS in comparison with both healthy tissue and other sarcomas. Our results support these data indicating that HDAC4 is elevated in aRMS cells.

HDAC4 is also a bona fide target of miR-206 (43) with miR-206 inhibiting expression of HDAC4 and augmenting histone acetylation (46). Moreover, miR-206 is not only a repressor of HDAC4 but also its downstream target.

Nuclear export of class IIa HDACs leads to derepression of target genes (44) and has been proposed as a mechanism regulating HDAC function. Nucleocytoplasmic shuttling of HDAC4 can be regulated by ROS (47). In the reduced state, HDAC domain

associates with the nuclear export signal (NES) and blocks its exposure to CRM1 exportin. After oxidation of Cys-667 and Cys-669, the HDAC domain dissociates from the NES, which is exposed to CRM1, inducing the nuclear export (46). Such mechanism has been described in lung carcinoma, where upon oxidation, HDAC4 was expulsed from the nucleus, leading to derepression of miR-206 (28). Enhanced nuclear export of HDAC4 and elevated miR-206 were described for Nrf2-deficient lung cancer, whereas when Nrf2 was active HDAC4 was localized in nucleus and miR-206 remained low (28).

Nrf2 is a transcription factor activated by oxidative stress to induce expression of antioxidant genes, such as *HMOX1* or *TRX1* (coding for thioredoxin-1). In cardiomyocytes, thioredoxin-1 regulates the HDAC4 translocation through the redox-dependent mechanism (47). Similar circuitry may be active in RMS to underlie the effect of HO-1 on miR-206. As we demonstrated in aRMS cells (with upregulated HO-1 and low ROS), HDAC4 is highly expressed and localized mainly in the nucleus. Inhibition of HO-1 promotes removal of HDAC4 from the nucleus, accompanied by upregulation of miR-206. Accordingly, reducing oxidative stress in eRMS cells (expressing low level of HO-1 and producing more ROS) leads to increased HDAC4 and decreased miR-206 production. Moreover, effect of HO-1 inhibition on miR-206, both *in vitro* and *in vivo*, is mimicked by valproic acid, inhibitor of HDACs, and by genetic knockdown of HDAC4.

HO-1 is an antioxidative enzyme, acting through removal of prooxidative heme and production of antioxidative biliverdin (16). Enzymatically inactive nuclear HO-1 may interact with Nrf2 to prevent its degradation. In murine fibroblasts, such interaction was required to induce antioxidant response (13). Our data reveal the presence of HO-1 both in cytoplasm and nucleus of RMS cells. Transfection with active and mutated form indicates that only active enzyme inhibits miR-206 expression.

Clinical relevance of miR-206 expression was shown in a cohort of RMS patients, where overall survival correlated with miR-206 level (8, 48). Apart from positive regulation of myogenesis-related factors, miR-206 inhibits cMET, leading to decreased RMS proliferation (28). Also, reconstitution of miR-206 caused a switch toward mature muscle and was capable of re-establishing differentiation in RMS (27). We demonstrate that such reconstitution, accompanied by decreased cell proliferation, is achieved by inhibition of HO-1.

miR-206 is regarded as a potentially druggable molecule, abrogating RMS growth in xenotransplant model (27) and inducing a switch toward the differentiated phenotype (49). Again, we observed the same effect in mice treated with HO-1 inhibitor. Moreover, inhibition of HO-1 was associated with decreased angiogenesis and augmented fibrosis, consistently with known proangiogenic and antifibrotic activities of HO-1 (50, 51). Our results show also that inhibition of HO-1 exclusively in RMS cells, despite upregulation of miR-206, is not sufficient to reduce the tumor growth, at least in aRMS type. The more reasonable approach seems the systemic pharmacologic inhibition of HO-1 affecting both RMS and stroma cells.

In summary, HO-1 is upregulated in aRMS cell lines and in tumors from patients with aRMS. Activation of HO-1 impedes myogenic differentiation of RMS by decreasing oxidative stress and possible preservation of reduced state of HDAC4 retained in the nucleus to repress miR-206. Inhibition of HO-1 downregulates CXCR4, SDF1, cMET, and HGF enhances myogenic differentiation, and may inhibit growth and vascularization of tumors. Our data suggest that inhibition of HO-1 might have a therapeutic potential in treatment of rhabdomyosarcoma.

Disclosure of Potential Conflicts of Interest

No potential conflicts of interest were disclosed.

Authors' Contributions

Conception and design: M. Ciesla, J. Dulak, A. Jozkowicz

Development of methodology: M. Jez, A. Szade, J. Stepniewski, J. Dulak, A. Jozkowicz

Acquisition of data (provided animals, acquired and managed patients, provided facilities, etc.): M. Ciesla, P. Marona, M. Kozakowska, M. Seczynska, A. Loboda, K. Bukowska-Strakova, A. Szade, M. Walawender, M. Kusior, K. Szade, B. Krist, O. Yagensky, A. Urbanik, B. Kazanowska, J. Dulak, A. Jozkowicz

Analysis and interpretation of data (e.g., statistical analysis, biostatistics, computational analysis): M. Ciesla, M. Kozakowska, M. Seczynska, A. Loboda, K. Bukowska-Strakova, M. Kusior, J. Dulak, A. Jozkowicz

Writing, review, and/or revision of the manuscript: M. Ciesla, B. Kazanowska, J. Dulak, A. Jozkowicz

Administrative, technical, or material support (i.e., reporting or organizing data, constructing databases): M. Kusior, A. Urbanik, J. Dulak

Study supervision: M. Ciesla, J. Dulak

Grant Support

The study was supported by grants from FNP (Ventures 2013-11/2, 2011-7/2 – M. Ciesla), NCN (2012/06/A/NZ1/00004, 2012/06/M/NZ1/00008, 2012/07/B/NZ1/02881 – A. Jozkowicz, J. Dulak), MNiSW (Iuventus Plus, IP2012 025572 – M. Kozakowska) by the EU FP POIG 01.02.00-069/09 and grant from NCBiR (PBS2/B7/15/2014 – J. Dulak, A. Jozkowicz, A. Loboda). Research was conducted in the scope of MiR-TANGO IAL (all authors). Faculty of Biochemistry, Biophysics and Biotechnology is beneficiary of KNOW grant (all authors).

The costs of publication of this article were defrayed in part by the payment of page charges. This article must therefore be hereby marked *advertisement* in accordance with 18 U.S.C. Section 1734 solely to indicate this fact.

Received July 13, 2015; revised June 19, 2016; accepted July 16, 2016; published OnlineFirst August 3, 2016.

References

1. Koscielniak E, Rodary C, Flamant F, Carli M, Treuner J, Pinkerton CR, et al. Metastatic rhabdomyosarcoma and histologically similar tumors in childhood: a retrospective European multi-center analysis. Med Pediatr Oncol 1992;20:209–14.
2. Newton WA Jr, Soule EH, Hamoudi AB, Reiman HM, Shimada H, Beltangady M, et al. Histopathology of childhood sarcomas. Intergroup Rhabdomyosarcoma Studies I and II: clinicopathologic correlation. J Clin Oncol 1988;1:67–75.
3. Casola S, Pedone PV, Cavazzana AO, Basso G, Luksch R, d'Amore ES, et al. Expression and parental imprinting of the H19 gene in human rhabdomyosarcoma. Oncogene 1997;14:1503–10.
4. Ahn EH. Regulation of target genes of PAX3-FOXO1 in alveolar rhabdomyosarcoma. Anticancer Res 2013;33:2029–35.
5. Walters ZS, Villarejo-Balcells B, Olmos D, Buist TW, Missiaglia E, Allen R, et al. JARID2 is a direct target of the PAX3-FOXO1 fusion protein and inhibits myogenic differentiation of rhabdomyosarcoma cells. Oncogene 2013;33:1148–57.
6. Tarnowski M, Grymula K, Liu R, Tarnowska J, Drukala J, Ratajczak J, et al. Macrophage migration inhibitory factor is secreted by rhabdomyosarcoma cells, modulates tumor metastasis by binding to CXCR4 and CXCR7 receptors and inhibits recruitment of cancer-associated fibroblasts. Mol Cancer Res 2010;8:1328–43.

7. Williamson D, Missiaglia E, de Reyniès A, Pierron G, Thuille B, Palenzuela G, et al. Fusion gene-negative alveolar rhabdomyosarcoma is clinically and molecularly indistinguishable from embryonal rhabdomyosarcoma. J Clin Oncol 2010;28:2151–8.
8. Keller C, Guttridge DC. Mechanisms of impaired differentiation in rhabdomyosarcoma. FEBS J 2013;280:4323–34.
9. Lassar AB, Davis RL, Wright WE, Kadesch T, Murre C, Voronova A, et al. Functional activity of myogenic HLH proteins requires hetero-oligomerization with E12/E47-like proteins in vivo. Cell 1991;66:305–15.
10. Wang H, Garzon R, Sun H, Ladner KJ, Singh R, Dahlman J, et al. NF-κB-YY1-miR-29 regulatory circuitry in skeletal myogenesis and rhabdomyosarcoma. Cancer Cell 2008;14:369–81.
11. Rota R, Ciarapica R, Giordano A, Miele L, Locatelli F. MicroRNAs in rhabdomyosarcoma: pathogenetic implications and translational potentiality. Mol Cancer 2011;10:120.
12. Kozakowska M, Ciesla M, Stefanska A, Skrzypek K, Was H, Jazwa A, et al. Heme oxygenase-1 inhibits myoblast differentiation by targeting myomirs. Antioxid Redox Signal 2012;16:113–27.
13. Biswas C, Shah N, Muthu M, La P, Fernando AP, Sengupta S, et al. Nuclear heme oxygenase-1 (HO-1) modulates subcellular distribution and activation of Nrf2, impacting metabolic and anti-oxidant defenses. J Biol Chem 2014;289:26882–94.
14. Was H, Dulak J, Jozkowicz A. Heme oxygenase-1 in tumor biology and therapy. Curr Drug Targets 2010;11:1551–70.
15. Balan M, Mier y Teran E, Waaga-Gasser AM, Gasser M, Choueiri TK, Freeman G, et al. Novel roles of c-Met in the survival of renal cancer cells through the regulation of HO-1 and PD-L1 expression. J Biol Chem 2015;290:8110–20.
16. Dulak J, Loboda A, Jozkowicz A. Effect of heme oxygenase-1 on vascular function and disease. Curr Opin Lipidol 2008;19:505–12.
17. Hjortsø MD, Andersen MH. The expression, function and targeting of haem oxygenase-1 in cancer. Curr Cancer Drug Targets 2014;14:337–47.
18. Galili N, Davis RJ, Fredericks WJ, Mukhopadhyay S, Rauscher FJ III, Emanuel BS, et al. Fusion of a fork head domain gene to PAX3 in the solid tumour alveolar rhabdomyosarcoma. Nat Genet 1993;5:230–5.
19. Kamimoto M, Mizuno S, Nakamura T. Reciprocal regulation of IL-6 and IL-10 balance by HGF *via* recruitment of heme oxygenase-1 in macrophages for attenuation of liver injury in a mouse model of endotoxemia. Int J Mol Med 2009;24:161–70.
20. Lin Q, Weis S, Yang G, Weng YH, Helston R, Rish K, et al. Heme oxygenase-1 protein localizes to the nucleus and activates transcription factors important in oxidative stress. J Biol Chem 2007;282:20621–33.
21. Chargé SB, Rudnicki MA. Cellular and molecular regulation of muscle regeneration. Physiol Rev 2004;84:209–38.
22. Ahn EH, Mercado GE, Laé M, Ladanyi M. Identification of target genes of PAX3-FOXO1 in alveolar rhabdomyosarcoma. Oncol Rep 2013;30:968–78.
23. Bennicelli JL, Edwards RH, Barr FG. Mechanism for transcriptional gain of function resulting from chromosomal translocation in alveolar rhabdomyosarcoma. Proc Natl Acad Sci U S A 1996;93:5455–9.
24. Ebauer M, Wachtel M, Niggli FK, Schäfer BW. Comparative expression profiling identifies an in vivo target gene signature with TFAP2B as a mediator of the survival function of PAX3/FKHR. Oncogene 2007;26:7267–81.
25. Sun L, Zhao Y, Gu S, Mao Y, Ji C, Xin X. Regulation of the *HMOX1* gene by the transcription factor AP-2δ with unique DNA binding site. Mol Med Rep 2014;10:423–8.
26. Gillespie MA, Le Grand F, Scimè A, Kuang S, von Maltzahn J, Seale V, et al. p38γ-dependent gene silencing restricts entry into the myogenic differentiation program. J Cell Biol 2009;187:991–1005.
27. Taulli R, Bersani F, Foglizzo V, Linari A, Vigna E, Ladanyi M, et al. The muscle-specific microRNA miR-206 blocks human rhabdomyosarcoma growth in xenotransplanted mice by promoting myogenic differentiation. J Clin Invest 2009;119:2366–78.
28. Singh A, Happel C, Manna SK, Acquaah-Mensah G, Carrerero J, Kumar S, et al. Transcription factor NRF2 regulates miR-1 and miR-206 to drive tumourigenesis. J Clin Invest 2013;123:2921–34.
29. Hou J, Dong J, Sun L, Geng L, Wang J, Zheng J, et al. Inhibition of phosphorylated c-Met in rhabdomyosarcoma cell lines by a small molecule inhibitor SU11274. J Transl Med 2011;9:64.
30. Anderson J, Ramsay A, Gould S, Pritchard-Jones K. PAX3-FKHR induces morphological change and enhances cellular proliferation and invasion in rhabdomyosarcoma. Am J Pathol 2001;159:1089–96.
31. Tapscott SJ, Lassar AB, Weintraub H. A novel myoblast enhancer element mediates MyoD transcription. Mol Cell Biol 1992;12:4994–5003.
32. Tajbakhsh S, Rocancourt D, Cossu G, Buckingham M. Redefining the genetic hierarchies controlling skeletal myogenesis: Pax-3 and Myf-5 act upstream of MyoD. Cell 1997;89:127–38.
33. Calhabeu F, Hayashi S, Morgan JE, Relaix F, Zammit PS. Alveolar rhabdomyosarcoma-associated proteins PAX3/FOXO1A and PAX7/FOXO1A suppress the transcriptional activity of MyoD-target genes in muscle stem cells. Oncogene 2013;32:651–62.
34. Sebire NJ, Malone M. Myogenin and MyoD1 expression in paediatric rhabdomyosarcomas. J Clin Pathol 2003;56:412–6.
35. Gagan J, Dey BK, Layer R, Yan Z, Dutta A. MicroRNA-378 targets the myogenic repressor MyoR during myoblast differentiation. J Biol Chem 2011;286:19431–8.
36. Megiorni F, Cialfi S, McDowell HP, Felsani A, Camero S, Guffanti A, et al. Deep sequencing the microRNA profile in rhabdomyosarcoma reveals down-regulation of miR-378 family members. BMC Cancer 2014;14:880.
37. Palacios D, Mozzetta C, Consalvi S, Caretti G, Saccone V, Proserpio V, et al. TNF/p38α/polycomb signaling to Pax7 locus in satellite cells links inflammation to the epigenetic control of muscle regeneration. Cell Stem Cell 2010;7:455–69.
38. Segalés J, Perdiguero E, Muñoz-Cánoves P. Epigenetic control of adult skeletal muscle stem cell functions. FEBS J 2015;282:1571–88.
39. Cesana M, Cacchiarelli D, Legnini I, Santini T, Sthandier O, Chinappi M, et al. A long noncoding RNA controls muscle differentiation by functioning as a competing endogenous RNA. Cell 2011;147:358–69.
40. Davis-Dusenbery BN, Hata A. MicroRNA in cancer: the involvement of aberrant microRNA biogenesis regulatory pathways. Genes Cancer 2010;1:1100–14.
41. Roccaro AM, Sacco A, Jia X, Azab AK, Maiso P, Ngo HT, et al. MicroRNA-dependent modulation of histone acetylation in Waldenstrom macroglobulinemia. Blood 2010;116:1506–14.
42. Lakshmaiah KC, Jacob LA, Aparna S, Lokanatha D, Saldanha SC. Epigenetic therapy of cancer with histone deacetylase inhibitors. J Cancer Res Ther 2014;10:469–78.
43. Winbanks CE, Wang B, Beyer C, Koh P, White L, Kantharidis P, et al. TGFβ regulates miR-206 and miR-29 to control myogenic differentiation through regulation of HDAC4. J Biol Chem 2011;286:13805–14.
44. Delcuve GP, Khan DH, Davie JR. Roles of histone deacetylases in epigenetic regulation: emerging paradigms from studies with inhibitors. Clin Epigenetics 2012;4:5.
45. Baird K, Davis S, Antonescu CR, Harper UL, Walker RL, Chen Y, et al. Gene expression profiling of human sarcomas: insights into sarcoma biology. Cancer Res 2005;65:9226–35.
46. Winbanks CE, Beyer C, Hagg A, Qian H, Sepulveda PV, Gregorevic P. MiR-206 represses hypertrophy of myogenic cells but not muscle fibers *via* inhibition of HDAC4. PLoS One 2013;8:e73589.
47. Ago T, Liu T, Zhai P, Chen W, Li H, Molkentin JD, et al. A redox-dependent pathway for regulating class II HDACs and cardiac hypertrophy. Cell 2008;133:978–93.
48. Missiaglia E, Shepherd CJ, Patel S, Thway K, Pierron G, Pritchard-Jones K, et al. MicroRNA-206 expression levels correlate with clinical behaviour of rhabdomyosarcomas. Br J Cancer 2010;102:1769–77.
49. Taulli R, Pandolfi PP. "Snorkeling" for missing players in cancer. J Clin Invest 2012;122:2765–8.
50. Stachurska A, Ciesla M, Kozakowska M, Wolffram S, Boesch-Saadatmandi C, Rimbach G, et al. Cross-talk between microRNAs, nuclear factor E2-related factor 2, and heme oxygenase-1 in ochratoxin A-induced toxic effects in renal proximal tubular epithelial cells. Mol Nutr Food Res 2013;57:504–15.
51. Sunamura M, Duda DG, Ghattas MH, Lozonschi L, Motoi F, Yamauchi J, et al. Heme oxygenase-1 accelerates tumor angiogenesis of human pancreatic cancer. Angiogenesis 2003;6:15–24.